J. Flow Injection Anal., Vol. 31, o. 1 (2014) 19-25

Track-Etched Microporous Membrane Electrodes and Its Applications in Flow Analysis

Hitoshi Mizuguchi

Graduate School of Science and Engineering, Yamagata University, 4-3-16, Jonan, Yonezawa, Yamagata 992-8510, Japan

This mini-review introduces electrochemical property and analytical applications of the track-etched microporous membrane electrodes. The electrodes were prepared by using a track-etched microporous membrane filter as a template which has a porous structure. The coating of platinum or gold was produced by sputter deposition onto both sides of the membrane filters. The electrode enables efficient electrolysis under a flow condition when the sample solution flows through the cylindrical pores of the electrode. Efficiency of electrolysis becomes remarkably higher by using the smaller pore size. This property would be attributed to the limitation of growth of the diffusion layer at the entrances of pores. Three-electrode and four-electrode system was fabricated by alternately piling up the electrodes and the membrane filters. Insertion of a membrane filter as a spacer between the electrodes avoids short-circuits and keeps a completely uniform distance between the electrodes. An immobilized enzyme reactor is also able to be mounted in the proposed electrode system. The simplicity and flexibility of arrangement of the electrodes as well as high efficiency of electrolysis is the greatest feature of the track-etched microporous membrane electrodes.

Keywords track-etched microporous membrane electrodes, flow cell, quantitative electrolysis, dual-electrode system, anodic stripping voltammetry, enzyme-based biosensor, FIA

1. Introduction

This mini-review focuses on fabrication of track-etched microporous membrane electrodes, construction of the flow cell in which the electrodes have been mounted, electrochemical property of the electrodes, and some applications of this electrode system.

The development of a flow cell which can produce quantitative electrolysis is attractive in the view of not only electrochemistry but also analytical or synthetic chemistry. To improve the efficiency of electrolysis, it is indispensable to enlarge the surface area of electrodes against the volume of solution, and the structure which can limit the growth of diffusion layer is also important [1].

The authors recently reported an electrochemical flow cell in which the track-etched microporous membrane electrodes had been mounted [2]. The electrode was prepared by sputter deposition of platinum or gold on the track-etched microporous membrane filters. The coatings were produced on the smooth flat surface and entrance of the cylindrical pores. The authors called this electrode as the track-etched microporous membrane electrode. A sample solution flows through the membrane filter while performing electrolysis. In this case, the sample solution flows through the cylindrical pores of the electrodes. The electrode described herein enables efficient electrolysis in a flow condition. This property would be attributed to the limitation of growth of the diffusion layer at the entrances of pores.

Track-etched membrane filter, which is produced by tracking process using thermal neutron bombardment and by chemical etching process, contains a smooth flat surface as well as cylindrical pores with uniform diameters [3,4]. The membrane filters are commercially available from 1970s, and the pores are defined precisely in the range from 0.01 to 10 μm order. Martin et al. described the preparation of ensembles of microscopic electrodes using this membrane filter as a template [5]. The authors used the membrane filter whose pore size was in the range from 0.4 to 5.0 μm. The sample solution can be flowed through the membrane filters even after piling up the membrane filters. Therefore, various analytical systems can be built by piling up the track-etched microporous membrane electrodes which have a 10 μm thickness. Although many researchers have investigated for quantitative electrolysis using a thin layer [6,7], column electrodes [8], or fiber-type electrodes [9,10], the simplicity and flexibility of arrangement of electrodes as well as high efficiency of electrolysis is the greatest feature of the track-etched microporous membrane electrodes.

In this article, fabrication of the electrochemical flow cell in which the track-etched microporous membrane electrodes have been mounted is described. Then, anodic stripping voltammetry equipped with the FIA system [11] and a series dual-electrode system [2] are introduced as applications of three- and four-electrode systems. An enzyme-based amperometric biosensor [12] as another application of the proposed flow cell is also described.

2. The track-etched microporous membrane electrodes

The membrane filters employed as a template of the

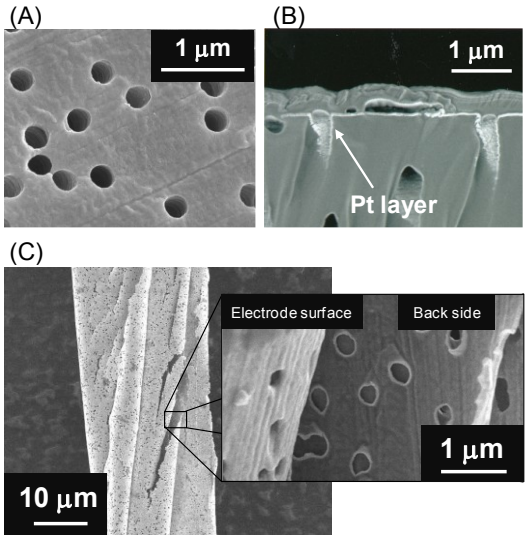

Fig. 1 SEM images of track-etched microporous membrane electrode produced by sputter deposition of platinum. (A) Surface of the electrode. (B) Cross sectional view. (C) The platinum layer which was exfoliated from the template filter by using *N*,*N*- dimethylformamide.

microporous membrane electrode were Nuclepore™ track-etched membrane filters (Whatman). The electrodes which were used in this study were fabricated by sputter deposition of platinum or gold onto both sides of the membrane filter using an auto fine coater (JFC-1600; JEOL Ltd.). Fig. 1 shows the SEM images of the microporous membrane electrode. The pore size of the template filter was 0.4 μm. Fig. 1 (A) is the surface of the membrane filter after producing of the coating of platinum. The existence of pores with uniform diameters is confirmed even after sputter deposition of platinum. Fig. 1 (B) shows a cross sectional view of the electrode. The smooth flat surface of the membrane filter and entrance of the cylindrical pores are modified with platinum. Fig. 1 (C) shows the platinum layer exfoliated from the template filter by using *N*,*N*-dimethylformamide. Shapes of the entrance of the cylindrical pores of the template filter were retained on the back side of the platinum layer. This is another evidence of the coating of platinum not only on the surface but also at the entrance of pores. The thickness of platinum layer can be controlled with the sputtering condition, such as current and deposition time. Stable electrochemical signals can be obtained using the electrodes with the thickness of the platinum layer of 70–100 nm because the membrane filter has a smooth flat surface.

3. Construction of the flow cell

The electrochemical flow-through cell fabricated in this study

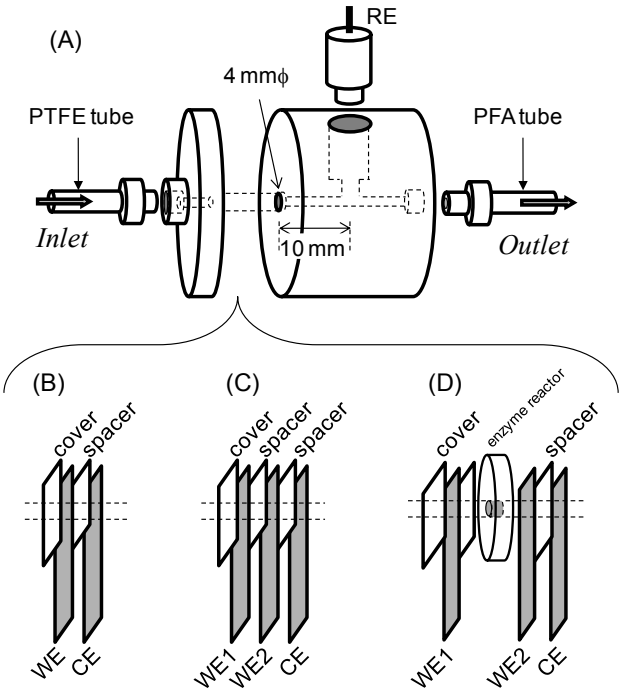

Fig. 2 Structure of the flow cell constructed in this study. (A) Main parts of the flow cell. (B) Three-electrode system. (C) Four-electrode system. (D) Four-electrode system in which an immobilized enzyme reactor is inserted.

is shown in Fig. 2. The electrodes prepared as noted above were cut into rectangular shape and placed in the flow channel by sandwiching between two parts of the flow cell which was made from a round bar of PEEK resin. Fig. 2 (B) and (C) show a three-electrode and a four-electrode system, respectively. Fig. 4 (D) shows the case where an immobilized enzyme reactor is inserted. These electrodes were alternately piled up with unmodified membrane filters. Insertion of an unmodified membrane filter as a spacer between the electrodes avoids short-circuits and keeps a completely uniform distance between the electrodes. The electrochemically active surface areas of the platinum electrodes whose pore sizes were 0.4, 1.0, and 5.0 μm were, respectively, 4.7, 4.2, and 4.1 cm^2 in the flow channel. A screw type reference electrode (silver-silver chloride in 3 M NaCl solution) was put at a 10 mm downstream of the counter electrode. Each electrode was connected to a bi-potentiostat or an electrochemical analyzer.

4. Anodic stripping voltammetry as an application of a three-electrode system –Ultra trace determination of Hg^{II}–

Anodic stripping voltammetry (ASV) is widely recognized as a powerful tool for measuring trace metals. The analyte of interest is electroplated on the working electrode during

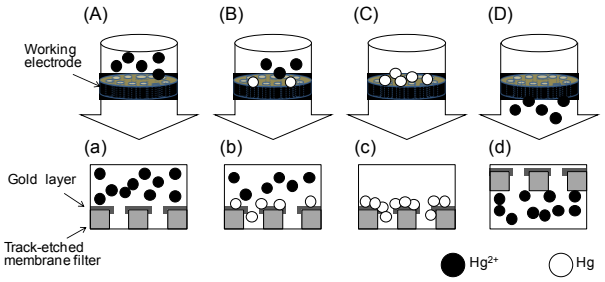

Fig. 3 Schematic representation of anodic stripping voltammetry with track-etched microporous membrane electrodes. Mercury is electrodeposited during flowing through the electrode (A–C) and oxidized during stripping (D). Cross sectional view (a–d).

deposition, and is oxidized from the electrode during stripping. The analyte can be detected by measuring the current in the stripping step. Mercury has been most widely known for several decades as an environmental pollutant. The WHO guideline value of mercury for drinking water quality is 1 μg l^{-1}. The concentration of mercury is regulated strictly all over the world. Consequently, extremely high sensitivity is necessary for mercury determination methods.

Many reports have described the detection and quantification of mercury by ASV, which are usually conducted after its electrolytic deposition on rotating [13], flow-through [14] or microwire [15] gold electrodes. The convective transport of the analyte to the electrode surface greatly benefits both enhancement of a substantial stripping signal and shortening the deposition time. In this study, the track-etched microporous membrane electrodes which enabled efficient electrolysis under a flow condition were employed to the FIA-ASV system for the determination of ultra-trace mercury(II) [11].

Schematic representation of the proposed method is shown in Fig. 3. Mercury is electrodeposited during flowing through the electrode, and oxidizes from the electrode during sweeping the potential in the positive direction. In the proposed system, the gold and platinum electrodes were employed as a working and a counter electrode, respectively. The flow cell was fabricated by piling the electrodes as shown in Fig. 2 (B). The slope of the calibration plots, which was obtained under the constant flow rate of 0.5 ml min^{-1}, became greater with increasing of the deposition time. A linear relation was observed between the analytical signals and the mercury(II) concentration at parts per billion levels. The detection limit for 180 s electrodeposition was 0.04 μg dm^{-3}. This value is comparable to the value obtained using the method with a wall-jet type electrochemical flow cell under continuous flow (8.0 ml min^{-1}) of the sample solution with electrodeposition time of 540 s [14]. The proposed method features low sample consumption and shorter electrodeposition time. Although the detection limit is often influenced by chemical modification or electrochemical polishing of the electrodes, the analytical performance described herein has supported efficient electrolysis using the track-etched microporous membrane electrode. The authors also demonstrated ASV with the sample injection mode using a 1-ml sample loop. The detection limit was 0.05 μg dm^{-3}. The gold electrode activity was maintained during at least 50 repetitions of mercury determination. This proposed method will become useful technique for on-site analyses after construction of an integral-type instrument.

5. Series dual-electrode system as an application of a four-electrode system

Dual-electrode system consists of two working electrodes [1]. In a series dual-electrode system, these electrodes are arranged in the direction of flow of sample solution. The potentials of these electrodes are controlled individually. The products generated by electrolysis at the first electrode (the generator electrode) are carried to the second electrode (the collector electrode) by a hydrodynamic flow. This electrode system is often called as a generator-collector mode. A rotating ring-disk electrode [16] and a channel flow double electrode [17] are well known as representative double electrode systems. These techniques have been also described theoretically [18–24]. Other dual-electrode systems available in electrochemistry include the wall-jet ring-disk electrode [25–28], a dual microband electrode [29,30], a dual micro-disk electrode [31,32], a twin interdigitated electrode [33–37], etc, with prosperousness of micro electrodes since the 1980s. These techniques have been largely used for investigating reaction mechanisms and related redox chemistry in various areas such as fuel cell, rechargeable battery, plating, corrosion, biomaterials, etc.

In flow analysis area, numerous reports have described various analytical techniques with a dual-electrode system [38–42] to eliminate interfering species prior to analytical steps [38–40], to generate titrating species for indirect detections [41], or to obtain signal amplification by means of redox cycling [38,40,42]. In these cases, the selectivity and sensitivity will increase with higher conversion efficiency of each electrode or higher collection efficiency of dual-electrode systems. In the conventional systems, it is expected the collection efficiency increases to nearly 100% with decreasing of the thickness of solution layer when large size electrodes are utilized in the lower

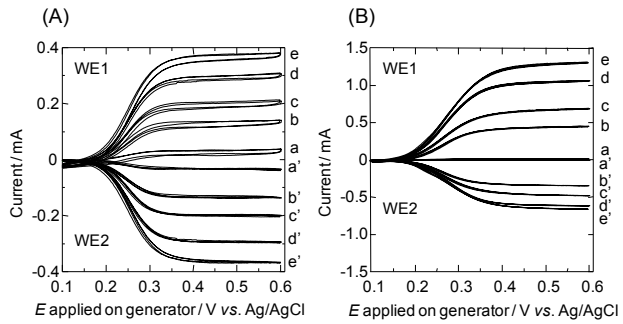

Fig. 4 Hydrodynamic voltammograms recorded at WE1 (a–e) and WE2 (a' –e'). (A) The pore size of the membrane filter was 0.4 μm. The concentration of hexacyanoferrate(II) ion was 0.30 mM. The velocities of sample solution were 0.09 (a, a'), 0.27 (b, b'), 0.43 (c, c'), 0.56 (d, d'), and 0.78 ml min^{-1} (e, e'). (B) The pore size was 5.0 μm. The concentration of hexacyanoferrate(II) ion was 1.0 mM. The velocities of sample solution were 0.14 (a, a'), 0.38 (b, b'), 0.68 (c, c'), 1.3 (d, d'), and 1.8 ml min^{-1} (e, e').

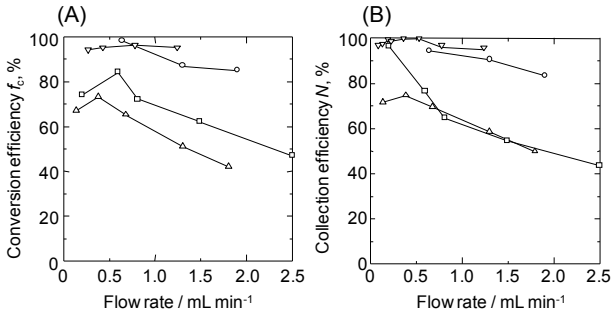

Fig. 5 Influence of the flow rate on the conversion efficiency (A) and collection efficiency (B).The pore size of the membrane filter used were 0.4 (▽), 1.0 (○), 3.0 (□), and 5.0 μm (△).

flow rate. However, when the flow rate or distances between the electrodes are extremely decreased, the problems such as diffusion of the material generated at the first electrode against the direction of flow will be caused [41,43]. Therefore, a flow cell which can keep high collection efficiency in a wide range of the flow rate would be really useful in flow analysis.

In this study, a dual-electrode system was fabricated by piling up the electrode as shown in Fig. 2 (C) [2]. The microporous membrane electrodes were sequentially arranged as the generator (WE1), collector (WE2), and counter electrode (CE) along with the flow direction of sample solution. The sample solution containing potassium hexacyanoferrate(II) was flowed into the electrochemical flow cell. The typical hydrodynamic voltammograms recorded at WE1 and WE2 are shown in Fig. 4. In this experiment, the potential of WE1 was swept between 0.1 and 0.6 V *vs*. Ag/AgCl, and the potential of WE2 was held at 0.1 V *vs*. Ag/AgCl. The characteristic sigmoidal responses were observed in both the voltammograms. The limiting current was greatly dependent on a pore size. When the pore size of the membrane filter used was 0.4 μm, the redox currents on both generator and collector electrodes were found to be proportional to the flow rate.

Fig. 5 shows flow rate dependences of conversion efficiency and collection efficiency. The conversion efficiency, which was calculated by Faraday's law, was increased with decreasing flow rate or smaller pore sizes employed. Greater than 96% of conversion efficiencies were obtained in the flow rate up to 1.2 ml min^{-1}, when the electrode of which pore size was 0.4 μm was used. The collection efficiencies, which are calculated by the ratio of the redox currents on both electrodes, tended similar to the conversion efficiency. Greater than 95% of the collection efficiencies were obtained with the electrode, whose template pore size was 0.4 μm, in the flow rate up to 1.2 ml min^{-1}. In spite of almost the same active area of these electrodes, there was a clear difference in the efficiency of electrolysis. This great contribution of pore size to the efficiency of electrolysis would be attributed to the limitation of growth of the diffusion layer at the entrances of pores. The amperometric response in a sample injection mode was also investigated. There was a very small delay between the anodic and the corresponding cathodic current. The maximum current, which is peak height, is proportional to concentration of the analyte. This result shows that signal amplification by redox-cycling will be employed in flow analysis systems.

The dual-electrode system described herein brings about high conversion efficiency and high collection efficiency in the relatively wide range of the flow rate. The authors emphasize the simple structure and easy fabrication as well as superior performance of this dual-electrode system.

6. Insertion of immobilized enzyme reactor into the four-electrode system –Flow-based biosensing system for glucose–

Enzyme-based amperometric biosensors are widely used for the determination of biomolecules in blood and food samples. Immobilized oxidase converts target analytes into hydrogen peroxide. Although hydrogen peroxide can be measured amperometrically, various organic compounds such as L-ascorbic acid and uric acid are co-oxidized and cause positive error in the indirect detection of biomolecules. To resolve this difficulty, different approaches using permselective membranes [44–47] or mediators with peroxidase in the probe [48,49] have been employed in the operation of enzyme electrodes, and some of

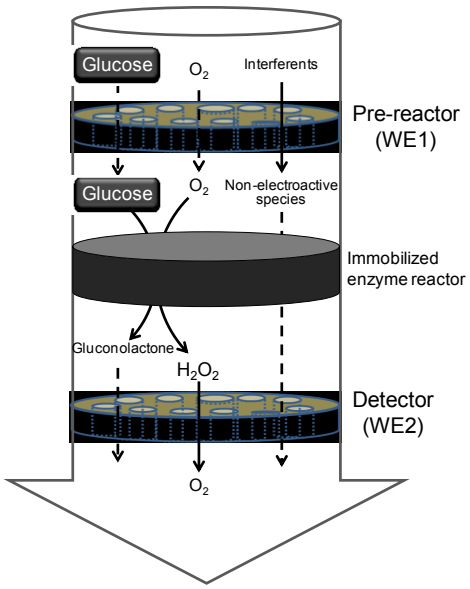

Fig. 6 Schematic representation of the principle of the proposed sensor system.

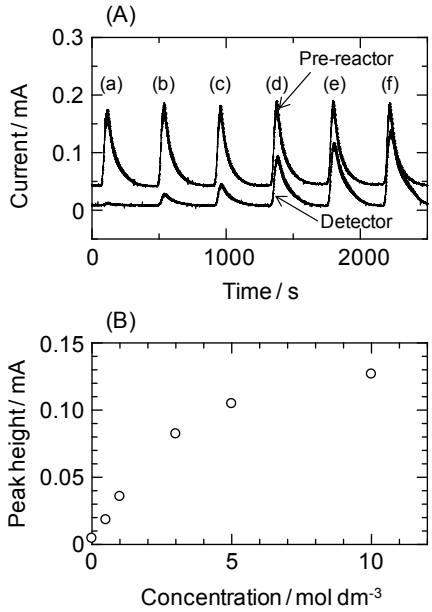

Fig. 7 (A) Flow signals for glucose at different concentrations. (B) The relation between glucose concentration and peak height at the detector electrode. Glucose concentrations were 0 (a), 0.5 (b), 1.0 (c), 3.0 (d), 5.0 (e), and 10.0 mM (f). Sample solutions contained 0.1 mM L-ascorbic acid, 0.2 mM uric acid, and 0.1 mM pyruvic acid.

these techniques have been put into practical use. On the other hand, removal of interfering species by pre-electrolysis is also compatible with an enzyme electrode incorporated in a flow system. The products of the electrolysis of the interferents such as L-ascorbic acid and uric acid are no longer electroactive because of its rapid hydrolysis. This approach is able to avoid some complicated procedures of surface modification of the electrodes. This strategy has been shown using a platinum tube electrode [50,51] a gold grid electrode [52], and a micro-fabricated electrochemical flow cell [53]. The biosensor selectivity is increased drastically by using these systems, but it is still difficult to remove the significant levels of interferents completely or at higher flow rates. As described in Section 4, greater than 96% of conversion efficiencies were obtained when the microporous membrane electrode of which pore size was 0.4 μm was used. In this study, the track-etched microporous membrane electrodes were employed to the amperometric biosensor for the specific detection of D-glucose (Fig. 6) [12].

The flow cell employed in this study was fabricated as shown in Fig. 2 (D). The electrodes made by producing the coating of platinum were used as a pre-reactor (WE1), a detector (WE2), and a counter electrode. In this study, efficiencies of electrolysis of L-ascorbic acid and uric acid were investigated before fabricating the enzyme-based biosensor. More than 96% of the substrates, such as 0.1 mM L-ascorbic acid or 0.2 mM uric acid, were electrolyzed during flowing through a membrane electrode. However, when the concentration of uric acid was 0.5 mM, the efficiencies were decreased somewhat gradually along with the increasing flow rate. To electrolyze the interferents at higher concentrations, the pre-reactor was produced by piling up two electrodes. As a result, more than 95% of uric acid at physiological concentrations, which resembled those in human blood, was eliminated by passing through the pre-reactor electrode in the range of flow rate up to 1.0 ml min^{-1}. This result shows that the proposed method is adoptable against different levels of interferents by introducing the pre-reactor with the piled electrodes.

The flow signals for D-glucose at different concentrations using sample injection mode are depicted in Fig. 7 (A). The amperometric response of the pre-reactor electrode at 0.9 V *vs.* Ag/AgCl derives from oxidation of the interferents and was independent of the glucose concentration. In contrast, the glucose-concentration-dependent responses were obtained at the detector electrode (Fig. 7 (B)). The detection limit of D-glucose under the condition of Fig. 7 was 1×10^{-4} mol dm^{-3}. Although the magnitude of an anodic current produced by the oxidation of hydrogen peroxide increases with increase of flow rate, the efficiency of enzymatic reaction decreases along with increase of the flow rate. Therefore the sensitivity of this proposed sensor system will be defined with these factors.

In the proposed system, selective detection of hydrogen peroxide generated by the enzymatic reaction was achieved with

no other catalytic material such as peroxidase or electron mediators. Simple structure and fabrication must be emphasized as well as its superior performance for biomolecule detection. Additionally, the present technique is well suited for the construction of a biosensor system using oxidases of different types. The proposed system will provide useful sensing devices having high sensitivity and selectivity.

7. Conclusions

As described in this review, high efficiency of electrolysis was brought about by using track-etched microporous membrane electrodes, which were fabricated by sputter deposition of platinum or gold. The coatings of platinum or gold were produced on the surface of the template membrane filters and entrances of the cylindrical pores. It is expected that the performance of the electrolysis is improved by using the electrode of which the coatings are produced at not only the entrances but also inner surfaces of the pores. Now the authors investigate the electrochemical property of the microporous membrane electrodes which is made by wet printing [54]. Furthermore, various analytical systems can be built merely by piling up the track-etched microporous membrane electrodes. The simplicity and flexibility of arrangement of electrodes as well as high efficiency of electrolysis must be emphasized as the greatest feature, which cannot be accomplished by conventional electrodes. Various useful systems will be provided by using the track-etched microporous membrane electrodes.

Acknowledgements

This work was supported by JSPS Grant-in-Aid for Scientific Research (No. 24550092), JSPS Grant-in-Aid for Young Scientists (No. 22750065), and was partially supported by the Foundation for Japanese Chemical Research. The authors also thank Mr. Noboru Imoto (technical staff member at Yamagata University) for helpful assistance in the flow cell construction.

References

[1] A. J. Bard, L. R. Faulkner, *Electrochemical Methods: Fundamentals and Applications second ed.*, 2001, Wiley, New York.

[2] H. Mizuguchi, K. Shibuya, A. Fuse, T. Hamada, M. Iiyama, K. Tachibana, T. Nishina, J. Shida, *Talanta*, **96**, 168–173 (2012).

[3] R. L. Fleischer, P. B. Price, R. M. Walker, *Nuclear Tracks in Solids, Principles and Applications*, University of California Press, Berkeley (1975).

[4] P. Apel, *Radiat. Meas.*, **34**, 559–566 (2001).

[5] M. Wirtz, S. Yu, C. R. Martin, *Analyst*, **127**, 871–879 (2002).

[6] K. Štulík, V. Pacáková, *J. Electroanal. Chem.*, **129**, 1–24 (1981).

[7] D.-I. Vaireanu, N. Ruck, P. R. Fielden, *Anal. Chim. Acta*, **306**, 115–122 (1995).

[8] W. J. Blaedel, J. H. Strohl, *Anal. Chem.*, **36**, 1245–1251 (1964).

[9] S. Kihara, *J. Electroanal. Chem.*, **45**, 31–44 (1973).

[10] A. N. Strohl , D. J. Curran, *Anal. Chem.*, **51**, 1045–1049 (1979).

[11] H. Mizuguchi, K. Numata, C. Monma, M. Iiyama, K. Tachibana, T. Nishina, J. Shida, *Anal. Sci.*, **29**, 949–954 (2013).

[12] H. Mizuguchi, J. Sakurai, Y. Kinoshita, M. Iiyama, T. Kijima, K. Tachibana, T. Nishina, J. Shida, *Chem. Lett.*, **42**, 1317–1319 (2013).

[13] Y. Bonfil, M. Brand, E. Kirowa-Eisner, *Anal. Chim. Acta*, **424**, 65–76 (2000).

[14] P. Richter, M. I. Toral, B. Abbott, *Electroanalysis*, **14**, 1288–1293 (2002).

[15] P. Salaün, C. M. G. van den Berg, *Anal. Chem.*, **78**, 5052–5060 (2006).

[16] A. Frumkin, L. Nekrasov, B. Levich, Ju. Ivanov, *J. Electroanal. Chem.*, **1**, 84–90 (1959).

[17] H. Gerischer, I. Mattes, R. Braun, *J. Electroanal. Chem.*, **10**, 553–567 (1965).

[18] H. Matsuda, *J. Electroanal. Chem.*, **16**, 153–164 (1968).

[19] R. Braun, *J. Electroanal. Chem.*, **19**, 23–35 (1968).

[20] K. Tokuda, H. Matsuda, *J. Electroanal. Chem.*, **44**, 199–212 (1973).

[21] K. Tokuda, H. Matsuda, *J. Electroanal. Chem.*, **52**, 421–431 (1974).

[22] K. Aoki, K. Tokuda, H. Matsuda, *J. Electroanal. Chem.*, **79**, 49–78 (1977).

[23] K. Aoki, H. Matsuda, *J. Electroanal. Chem.*, **94**, 157–163 (1978).

[24] K. Aoki, K. Tokuda, H. Matsuda, *J. Electroanal. Chem.*, **195**, 229–249 (1985).

[25] W. J. Albery, C. M. A. Brett, *J. Electroanal. Chem.*, **148**, 201–210 (1983).

[26] W. J. Albery, C. M. A. Brett, *J. Electroanal. Chem.*, **148**, 211–220 (1983).

[27] R. G. Compton, A. C. Fisher, M. H. Latham, C. M. A. Brett,

A. M. C. F. Oliveira Brett, *J. Appl. Electrochem.*, **22**, 1011–1016 (1992).

[28] K. Toda, S. Oguni, Y. Takamatsu, I. Sanemasa, *J. Electroanal. Chem.*, **479**, 57–63 (1999).

[29] J. E. Bartelt, M. R. Deakin, C. Amatore, R. M. Wightman, *Anal. Chem.*, **60**, 2167–2169 (1988).

[30] H. Rajantie, J. Strutwolf, D. E. Williams, *J. Electroanal. Chem.*, **500**, 108–120 (2001).

[31] J. E. Baur, P. N. Motsegood, *J. Electroanal. Chem.*, **572**, 29–40 (2004).

[32] I. J. Cutress, Y. Wang, J. G. Limon-Petersen, S. E. C. Dale, L. Rassaei, F. Marken, R. G. Compton, *J. Electroanal. Chem.*, **655**, 147–153 (2011).

[33] D. G. Sanderson, L. B. Anderson, *Anal. Chem.*, **57**, 2388–2393 (1985).

[34] A. J. Bard, J. A. Crayston, G. P. Kittlesen, T. V. Shea, M. S. Wrighton, *Anal. Chem.*, **58**, 2321–2331 (1986).

[35] C. E. Chidsey, B. J. Feldman, C. Lundgren, R. W. Murray, *Anal. Chem.*, **58**, 601–607 (1986).

[36] K. Aoki, M. Morita, O. Niwa, H. Tabei, *J. Electroanal. Chem.*, **256**, 269–282 (1988).

[37] O. Niwa, M. Morita, H. Tabei, *Anal. Chem.*, **62**, 447–452 (1990).

[38] A. Aoki, T. Matsue, I. Uchida, *Anal. Chem.*, **62**, 2206–2210 (1990).

[39] M. Zhao, D. B. Hibbert, J. J. Gooding, *Anal. Chem.*, **75**, 593–600 (2003).

[40] K. Hayashi, Y. Iwasaki, R. Kurita, K. Sunagawa, O. Niwa, A. Tate, *J. Electroanal. Chem.*, **579**, 215–222 (2005).

[41] T. R. L. C. Paixão, R. C. Matos, M. Bertotti, *Electochim. Acta*, **48**, 691–698 (2003).

[42] H. Tabei, M. Takahashi, S. Hoshino, O. Niwa, T. Horiuchi, *Anal. Chem.*, **66**, 3500–3502 (1994).

[43] C. Amatore, N. Da Mota, C. Lemmer, C. Pebay, C. Sella, L. Thouin, *Anal. Chem.*, **80**, 9483–9490 (2008).

[44] J. Wang, T. Golden, *Anal. Chem.*, **61**, 1397–1400 (1989).

[45] S. V. Sasso, R. J. Pierce, R. Walla, A. M. Yacynych, *Anal. Chem.*, **62**, 1111–1117 (1990).

[46] S.-K. Jung, G. S. Wilson, *Anal. Chem.*, **68**, 591–596 (1996).

[47] F. Mizutani, S. Yabuki, Y. Hirata, *Anal. Chim. Acta*, **314**, 233–239 (1995).

[48] M. Vreeke, R. Maidan, A. Heller, *Anal. Chem.*, **64**, 3084–3090 (1992).

[49] O. Niwa, R. Kurita, T. Horiuchi, K. Torimitsu, *Anal. Chem.*, **70**, 89–93 (1998).

[50] A. Koshy, E. Zilkha, T. P. Obrenovitch, H. P. Bennetto, D. A. Richards, L. Symon, *Anal. Lett.*, **26**, 831–849 (1993).

[51] P. G. Osbone, O. Niwa, T. Kato, K. Yamamoto, *Curr. Sep.*, **15**, 19–23 (1996).

[52] N. C. Bacon, E. A. H. Hall, *Electroanalysis*, **11**, 749–755 (1999).

[53] K. Hayashi, R. Kurita, T. Horiuchi, O. Niwa, *Electroanalysis*, **14**, 333–338 (2002).

[54] S. Sato, T. Sato, G. Hayakawa, H. Mizuguchi, *The 62nd annual meeting of JSAC*, Y1035, Higashi-Osaka (2013).

(Received June 18, 2014)
(Accepted June 24, 2014)